

# SEMI-INTRUSIVE UNCERTAINTY QUANTIFICATION FOR MULTISCALE MODELS

ANNA NIKISHOVA<sup>1</sup> AND ALFONS G. HOEKSTRA<sup>1,2</sup>

<sup>1</sup>*Computational Science Lab, Institute for Informatics, Faculty of Science, University of Amsterdam, The Netherlands*

<sup>2</sup>*ITMO University, Saint Petersburg, Russia*

**ABSTRACT.** We propose a family of semi-intrusive Uncertainty Quantification (UQ) methods for multiscale models with separated time scales. The methods are semi-intrusive in the sense that we limit the inspection of the multiscale model up to the level of the single scale systems. Our goal was to reduce the computation time spent on UQ of micro-scale models, since they usually represent the computationally most intensive part of multiscale models. Moreover, micro-scale models are usually executed at every time step of the slow dynamics, adding even more to their contribution to overall computing time. We tested the semi-intrusive algorithms on two case studies based on reaction-diffusion dynamics. Comparison of the UQ approaches shows that the proposed semi-intrusive methods can result in a significant reduction of the computational time, while still computing accurate estimates of uncertainties.

## 1. INTRODUCTION

Computer modeling is widely used in science and engineering to study systems of interest and to predict their behaviour. These systems are usually multiscale in nature, as their accuracy and reliability depend on the correct representation of processes taking place on several length and time scales [11, 14, 16, 20, 28]. Such multiscale systems are usually stochastic, since there are always some unresolved scales, which effects are not taken into account due to lack of knowledge or limitations of computational power [2, 20]. Moreover, measurements of model parameters, model validation, or initial and boundary conditions can never be made with perfect accuracy, thus, such data inevitably contain uncertainties [18].

We distinguish between intrusive UQ methods, where we need to modify the model by its stochastic representation, and non-intrusive methods, where the original model is used as a black-box [21, 29]. Intrusive methods are efficient and relatively easy to apply to linear models [33]. This, however, represents only a relative small class of models. They can be applied to non-linear models as well, but solution of the resulting equations may become very demanding [36]. non-intrusive methods can be applied to any type of non-linear model. However, these methods usually require a very large number of model runs [12], which may prohibit using such non-intrusive methods.

Our ultimate aim is to design an efficient algorithm for Uncertainty Quantification (UQ) for Multiscale models. We have developed a generic Multi Scale Modelling and Simulation Framework (MMSF) [4–6, 8], where a Multiscale model is represented as a collection of coupled single scale models. In this paper, we show that, given the structure of a multiscale model, we are able to perform UQ more efficiently in comparison with

---

*E-mail address:* A.Nikishova@uva.nl, A.G.Hoekstra@uva.nl.

non-intrusive approaches, keeping at the same time a high confidence in the results of UQ. We intend to integrate the semi-intrusive UQ algorithms proposed here with the MMSF.

In this paper, we discuss and test a family of semi-intrusive UQ approaches. In contrast to [1] and [22], in our semi-intrusive approaches there is no need to perform any modification of the single scale model solvers. On the contrary, we use information about the multiscale model structure, and the methods are intrusive only on the level of the multiscale model. First, we propose a semi-intrusive Monte Carlo (SIMC) method for multiscale models with separated temporal scales, where we reduce the number of samples for the computationally intensive part of the multiscale model, i.e. usually the micro scale model (the fast dynamics). In the second proposed approach, we constructed a metamodel for the computationally expensive single scale model. In the third method, we consider the situation, when we are able to substitute a single scale model by its stochastic representation, and we discuss in some details the stochastic Galerkin method coupled with non-intrusive Polynomial Chaos.

We tested our methods on two case studies based on reaction-diffusion dynamics with random inputs: a one-dimensional system and the Gray-Scott model with slow diffusion and fast reaction. We conclude that the proposed methods result in a significant decrease of computational time. Moreover, applying the SIMC method, we are able to control the error from the interpolation, which was an important point in the second case study.

The paper is organized as follows. In section 2, we briefly discuss the multiscale modelling and time splitting. The proposed UQ algorithms are presented in section 3. The results from two case studies are in section 4 and section 5, and the conclusions follow in section 6.

## 2. MULTISCALE MODEL

Before a computational model is built, a mathematical description of the process should be found and approximated by a numerical method. Let us consider a partial differential equation (PDE), which describes the process we are interested in and has the form

$$\begin{aligned} \frac{\partial u(x, t, \xi)}{\partial t} &= \mathcal{L}(u(x, t, \xi), \xi), \text{ for } t > 0 \\ u(x, t = 0) &= u_0 \end{aligned} \quad (1)$$

with homogeneous or periodic boundary conditions.  $x$  and  $t$  are space and time variables,  $\mathcal{L}$  is an operator acting in the space variable, and  $u$  is the quantity of interest (QoI), which evolution in time is studied.  $\xi \in [0, 1]^n$  denotes a  $n$ -dimensional space of uncertain input.

The analytical solution of Eq. 1 satisfies

$$u(x, t, \xi) = e^{t\mathcal{L}} u_0. \quad (2)$$

**2.1. Operator splitting.** Operator splitting is an efficient technique for decomposition of a complex model into a sequence of sub-systems, which is easier to simulate, for instance, applying different and more appropriate numerical approaches for each of the sub-problems.

Let us assume for  $\mathcal{L}$  a two-term splitting:

$$\mathcal{L} = \mathcal{L}^A + \mathcal{L}^B. \quad (3)$$

Thus, Eq. 2 can be approximated by

$$u(x, t, \xi) \approx e^{t\mathcal{L}^B} e^{t\mathcal{L}^A} u_0. \quad (4)$$

Eq. 1 is approximated as a sequence of the following two sub-systems [17]

$$\begin{aligned} \frac{\partial u^*(x, t, \xi)}{\partial t} &= \mathcal{L}^A(u^*(x, t, \xi), \xi), \text{ for } t_n < t < t_{n+1}, \\ &\text{with } u^*(x, t_n, \xi) \approx u(x, t_n, \xi), \\ \frac{\partial u^{**}(x, t, \xi)}{\partial t} &= \mathcal{L}^B(u^{**}(x, t, \xi), \xi), \text{ for } t_n < t < t_{n+1}, \\ &\text{with } u^{**}(x, t_n, \xi) = u^*(x, t_{n+1}, \xi). \end{aligned} \quad (5)$$

In the case of commuting operators (i.e.  $\mathcal{L}^A \mathcal{L}^B = \mathcal{L}^B \mathcal{L}^A$ ), replacing Eq. 1 and 2 by Eq. 4 and 5 is exact. Otherwise, it produces a *splitting error*, which can be reduced by applying high-order time-splitting schemes (see, e.g. [9, 17, 22, 32]).

**2.2. Splitting fast from slow.** In this study, we investigate systems with operators on different time scales. In such cases, time splitting methods are used to speed up computations, since only "fast" processes should be computed with a fine time scale, and the rest of the operators we can use a coarser time scale.

Let us assume for  $\mathcal{L}$  a two-term splitting [11]:

$$\mathcal{L} = \frac{1}{\epsilon} \mathcal{L}^f + \mathcal{L}^s, \quad (6)$$

where  $0 < \epsilon \ll 1$  quantifies the time scale separation,  $\mathcal{L}^f$  and  $\mathcal{L}^s$  are operators of fast and slow dynamics<sup>1</sup>, respectively. In other words, the fast dynamics evolves the system to a local equilibrium state much faster than the evolution of the slow dynamics. Methods like quasi-steady state approximations average the fast processes to solve the fast and slow dynamics on different temporal scales and to obtain a multiscale model [25]. We assume that the update of the quantity of interest ( $u^t$ ) using a discretion scheme can be represented as

$$\begin{aligned} u^{t+\Delta t_\mu}(\xi) &= F^f(u^t(\xi), \xi, \Delta t_\mu), \\ u^{t+\Delta t_M}(\xi) &= F^s(u^{t+n_1\Delta t_\mu}(\xi), \xi, \Delta t_M), \end{aligned} \quad (7)$$

where  $F^f$  is a function, which updates the state variable according to  $\mathcal{L}^f$  with a micro time step  $\Delta t_\mu$ , and  $F^s$  updates the result from the micro model  $u^{t+n_1\Delta t_\mu}$  according to the slow dynamics given by  $\mathcal{L}^s$  with a macro time step  $\Delta t_M$ , and  $n_1 \leq \frac{\Delta t_M}{\Delta t_\mu}$  is the number of iterations of the micro scale model.

In general, a model with two or more different time scales can be illustrated by a *Submodel Execution Loop* as defined in the context of the MMSF [6]. In Figure 1a, we show an example with two different time scales, where  $u_{init}$  are some initial conditions for a single scale model,  $O$  is the observation of the current state,  $S$  is the solver, and  $B$  is the application of boundary conditions. More information about the submodel execution loops can be found in [5, 8]. Later in the text, we represent a multiscale model as a collection of coupled single scale models (Figure 1b), where the horizontal arrows denote the model initialisation and the submission of the final result, and the vertical arrows denote the exchange of the information between single scale models.

The execution time of the multi-scale model is

$$T_{model} = n_2(n_1\gamma + \beta), \quad (8)$$

---

<sup>1</sup>Note that, in theory, each of the fast and slow operators can be splitted again, in the case of more than two processes.

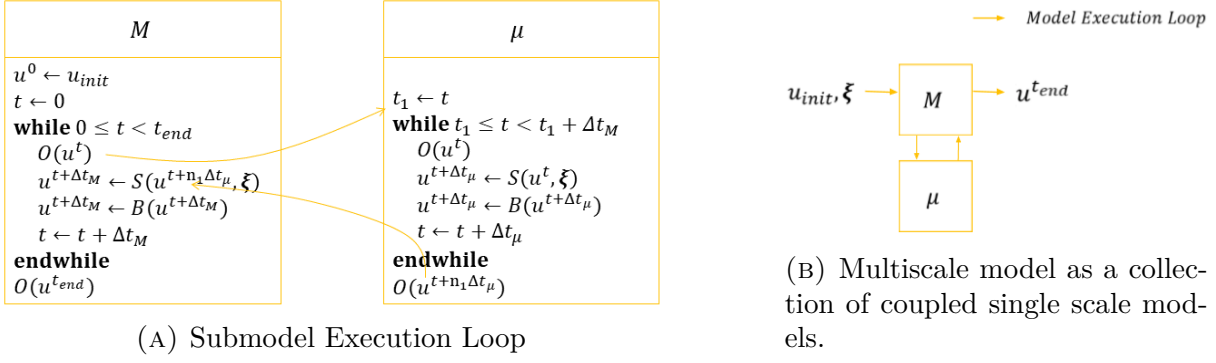


FIGURE 1. Structure of a multiscale model. Here and later in the text,  $M$  denotes the macro model, and  $\mu$  stands for the micro model.

where  $n_2 = \frac{t_{end}}{\Delta t_M}$  is the number of iterations of the macro scale model,  $n_1$  is the number of iterations of the micro scale model,  $\gamma$  and  $\beta$  are the computational time of one iteration of the micro and macro model, respectively.

### 3. UNCERTAINTY QUANTIFICATION

In this section, we show how we can decrease the computational time of uncertainty quantification by exploiting the structure of the multiscale model. The computational time of the algorithms is compared with the execution time of a plain Monte Carlo method.

**3.1. Plain Monte Carlo.** To find the mean value and variance of the model response with a Monte Carlo (MC) method, one needs to run the model  $N$  times with different values of uncertain model inputs  $\xi$ :

$$\begin{aligned}
 \mathbb{E}[u^{t+\Delta t_M}(\xi)] &= \int_{(0,1)^n} \left( F^s(u^{t+n_1\Delta t_\mu}(\xi), \xi, \Delta t_M) \right) d\xi \\
 &\approx \frac{1}{N} \sum_{j=0}^{N-1} \left( F^s(u_j^{t+n_1\Delta t_\mu}(\xi_j), \xi_j, \Delta t_M) \right), \\
 \mathbb{E}[(u^{t+\Delta t_M}(\xi))^2] &\approx \frac{1}{N} \sum_{j=0}^{N-1} \left( F^s(u_j^{t+n_1\Delta t_\mu}(\xi_j), \xi_j, \Delta t_M) \right)^2, \\
 Var[u^{t+\Delta t_M}(\xi)] &= \mathbb{E}[(u^{t+\Delta t_M}(\xi))^2] - \mathbb{E}^2[u^{t+\Delta t_M}(\xi)],
 \end{aligned} \tag{9}$$

where  $u_i^{t+n_1\Delta t_\mu}(\xi_j)$  denotes the micro model response given the vector of model parameters  $\xi_j$ .

In Figure 2 we schematically show the resulting algorithm. First, we generate  $N$  samples of uncertain inputs denoted by  $\xi$ . Then, we run the model  $N$  times and sample the model outcome, in order to compute model uncertainty.

The computational time of running the MC method for the multi-scale model is

$$T_{MC} = NT_{model} = N(n_2(n_1\gamma + \beta)). \tag{10}$$

**3.2. Semi-intrusive Monte Carlo.** Our first attempt to decrease UQ computational time is to change the order of model execution and UQ loops (Figure 3 with  $N_1 = N$ ). Eq. 9 is still valid for the model response uncertainty estimation and the computational time of running the MC method with the change of loops order is the same:

$$T_{MCex} = n_2(Nn_1\gamma + N\beta) = T_{MC}. \tag{11}$$

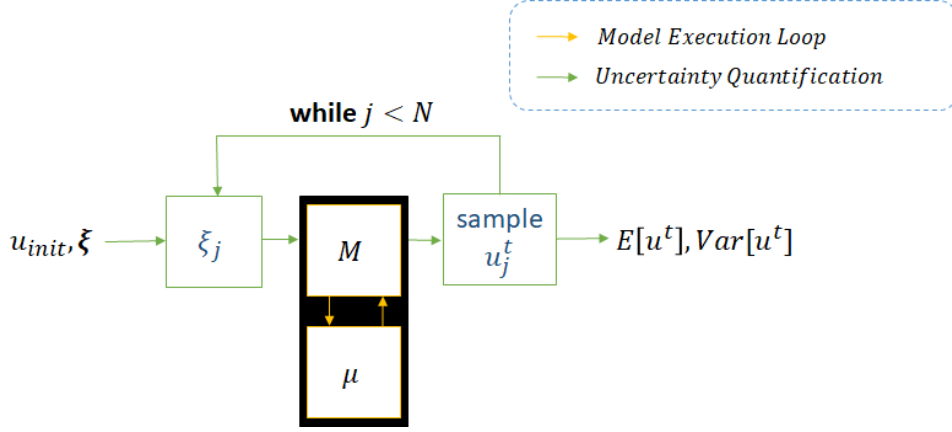


FIGURE 2. Monte Carlo method

However, at this point, we are able to set a different number of samples for the micro and macro model (Figure 3). Definitely, to speed up calculations, we can set this number to be much less for the micro model. Let us denote the number of MC samples for the micro model by  $N_1$ , and  $N$  be the number of MC samples for macro model with  $N > N_1$ . The initial state for the macro model for samples  $i$ , such that  $N_1 \leq i < N$ , can be obtained using regression or interpolation methods. Thus, the mean value can be approximated by

$$\mathbb{E}[u^{t+\Delta t_M}(\xi)] \approx \frac{1}{N} \left( \sum_{j=0}^{N_1-1} F^s(u_j^{t+n_1\Delta t_\mu}(\xi_j), \xi_j, \Delta t_M) + \sum_{j=N_1}^{N-1} (F^s(\tilde{u}_j^{t+n_1\Delta t_\mu}(\xi_j), \xi_j, \Delta t_M)) \right), \quad (12)$$

where  $\tilde{u}_j^{t+n_1\Delta t_\mu}(\xi_j)$  denotes the results of interpolation of the micro model output with input  $\xi_j$ .

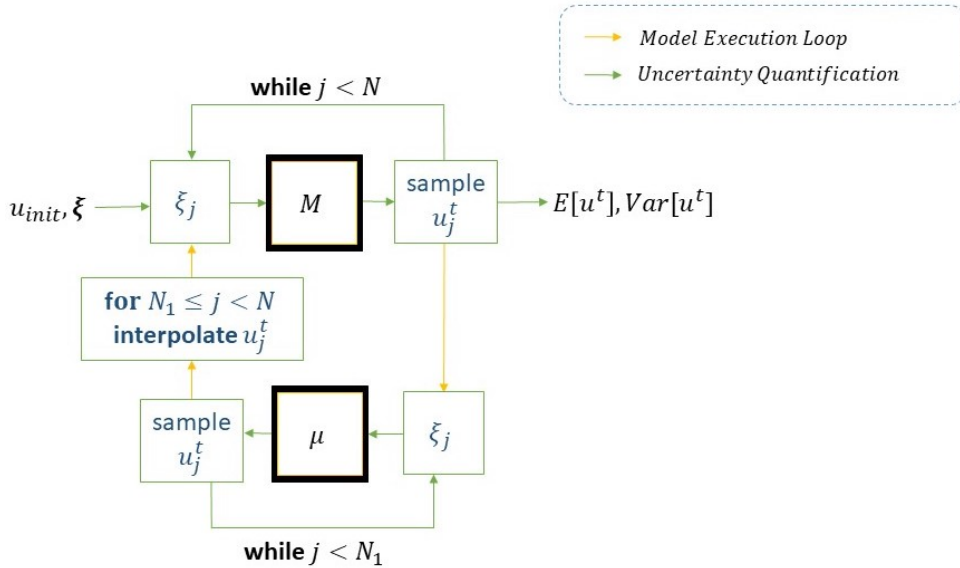


FIGURE 3. Semi-intrusive Monte Carlo method with a smaller number of samples of the expensive micro scale model

The computational time of running the Monte Carlo method separately on different model time scales is

$$T_{SIMC} = n_2(N_1 n_1 \gamma + N \beta) + \varepsilon, \quad (13)$$

where  $\varepsilon$  is the computational time of interpolation.

The gain in computational cost in comparison with the black box approach is

$$T_{MC} - T_{SIMC} = n_2 n_1 \gamma (N - N_1) - \varepsilon. \quad (14)$$

It is clear that we introduce an error by taking a smaller sample size for the micro level. Thus, we need to perform an interpolation test in order to estimate how good the micro model approximation is.

**3.2.1. Interpolation test.** On each macro time step we have to find out whenever the approximation of the micro model does not produce large error in the statistical quantities of the macro model result, namely we want to minimize the following values

$$\begin{aligned} \min |\mathbb{E}[u^{t+\Delta t_M}] - \mathbb{E}[\tilde{u}^{t+\Delta t_M}]|, \\ \min |\sigma_{u^{t+\Delta t_M}} - \sigma_{\tilde{u}^{t+\Delta t_M}}|, \end{aligned} \quad (15)$$

where  $\sigma_u = \sqrt{\text{Var}[u]}$  is the standard deviation.

Let us denote by  $f_{0,\dots,n-1}(\xi_n)$  the interpolation of  $n$ -th point using the set of original micro model outputs  $u_0^{t+n_1\Delta t_\mu}, u_1^{t+n_1\Delta t_\mu}, \dots, u_{n-1}^{t+n_1\Delta t_\mu}$ . We call  $\tilde{u}_0^{t+n_1\Delta t_\mu}, \tilde{u}_1^{t+n_1\Delta t_\mu}, \dots, \tilde{u}_{N_1-1}^{t+n_1\Delta t_\mu}$  the interpolation results of the micro model output, such that

$$\begin{aligned} \tilde{u}_0^{t+n_1\Delta t_\mu} &= f_{1,\dots,N_1-1}(\xi_0), \\ \tilde{u}_1^{t+n_1\Delta t_\mu} &= f_{0,2,\dots,N_1-1}(\xi_1), \\ &\dots \\ \tilde{u}_{N_1-1}^{t+n_1\Delta t_\mu} &= f_{0,\dots,N_1-2}(\xi_{N_1-1}). \end{aligned} \quad (16)$$

In other words, we interpolated already sampled points  $\tilde{u}_j^{t+n_1\Delta t_\mu}$  for  $0 \leq j < N_1$  using the rest of the sample  $\{u_i^{t+n_1\Delta t_\mu} : 0 \leq i < N_1, i \neq j\}$  with the function  $f_{0,\dots,N_1}(\xi_j)$ . The outputs of the macro model with the initial value that results from the interpolation are denoted by  $\tilde{u}_0^{t+\Delta t_M}, \dots, \tilde{u}_{N_1-1}^{t+\Delta t_M}$ . Comparing the statistics obtained from the original and the interpolated sets, we want to test whether  $N_1$  points are sufficient to construct the interpolation of the micro model output or if we have to increase the number of sample points.

First, we bound the values in Eq. 15 by

$$|\mathbb{E}[u^{t+\Delta t_M}] - \mathbb{E}[\tilde{u}^{t+\Delta t_M}]| \leq \mathbb{E}[|u^{t+\Delta t_M} - \tilde{u}^{t+\Delta t_M}|] \quad (17)$$

Then, we set the error in the mean value of the model output with interpolation input be within a factor  $\zeta$  of the standard deviation

$$\frac{1}{N_1} \sum_{i=0}^{N_1-1} |u_i^{t+\Delta t_M} - \tilde{u}_i^{t+\Delta t_M}| \leq \zeta \cdot s_u, \quad (18)$$

where

$$s_u = \sqrt{\frac{1}{N_1 - 1} \sum_{i=0}^{N_1-1} (u_i^{t+\Delta t_M} - \bar{u})^2}$$

is the sample standard deviation,

$$\bar{u} = \frac{1}{N_1} \sum_{i=0}^{N_1-1} u_i^{t+\Delta t_M}$$

is the sample mean, and  $0 < \zeta < 1$  is a required accuracy. In other words, we want that the approximation error is much less than the variability of the function itself.

In a similar way, we bound the error in the standard deviation:

$$|\sigma_{u^{t+\Delta t_M}} - \sigma_{\tilde{u}^{t+\Delta t_M}}| \leq \sigma_{|u^{t+\Delta t_M} - \tilde{u}^{t+\Delta t_M}|} \quad (19)$$

This inequality can be proved applying the Cauchy-Schwarz inequality.

We set the error in the standard deviation to be less than the estimated standard deviation from the  $N_1$  original sample points

$$s_{|u^{t+\Delta t_M} - \tilde{u}^{t+\Delta t_M}|} \leq \eta s_u, \quad (20)$$

where  $0 < \eta < 1$  is a required accuracy for the standard deviation.

In this way, the confidence interval of the error estimate is bounded with  $s_{u^{t+\Delta t_M}}$

$$\begin{aligned} \left| \mathbb{E}[|u^{t+\Delta t_M} - \tilde{u}^{t+\Delta t_M}|] - \frac{1}{N_1} \sum_{i=0}^{N_1-1} |u_i^{t+\Delta t_M} - \tilde{u}_i^{t+\Delta t_M}| \right| &\leq \frac{z^* s_{|u^{t+\Delta t_M} - \tilde{u}^{t+\Delta t_M}|}}{\sqrt{N_1}} \\ &\leq \frac{z^*}{\sqrt{N_1}} \eta s_u, \\ \left| \sigma_{|u^{t+\Delta t_M} - \tilde{u}^{t+\Delta t_M}|} - s_{|u^{t+\Delta t_M} - \tilde{u}^{t+\Delta t_M}|} \right| &\leq \left( \sqrt{\frac{N_1 - 1}{\chi_{\alpha/2}^2}} - \sqrt{\frac{N_1 - 1}{\chi_{1-\alpha/2}^2}} \right) s_{|u^{t+\Delta t_M} - \tilde{u}^{t+\Delta t_M}|} \\ &\leq \left( \sqrt{\frac{N_1 - 1}{\chi_{\alpha/2}^2}} - \sqrt{\frac{N_1 - 1}{\chi_{1-\alpha/2}^2}} \right) \eta s_u, \end{aligned} \quad (21)$$

where  $z^*$ ,  $\chi_{1-\alpha/2}^2$  and  $\chi_{\alpha/2}^2$  are the points of the probability density function, denoting the probability to observe a larger value and defined only by the confidence level and  $N_1$ . Therefore, the estimated error from the interpolation test with  $N_1$  samples can tell us approximately the error we will have when we interpolate  $N - N_1$  points using same interpolation function  $f_{0,\dots,n-1}(\xi_n)$ .

Let us now consider the ratio

$$\begin{aligned} \left( \frac{s_{|u^{t+\Delta t_M} - \tilde{u}^{t+\Delta t_M}|}}{s_u} \right)^2 &= \frac{\mathbb{E}[(u^{t+\Delta t_M} - \tilde{u}^{t+\Delta t_M})^2] - \mathbb{E}^2[|u^{t+\Delta t_M} - \tilde{u}^{t+\Delta t_M}|]}{\mathbb{E}[(u^{t+\Delta t_M})^2] - \mathbb{E}^2[u^{t+\Delta t_M}]} \\ &\leq \frac{\mathbb{E}[(u^{t+\Delta t_M} - \tilde{u}^{t+\Delta t_M})^2]}{\mathbb{E}[(u^{t+\Delta t_M})^2] - \mathbb{E}^2[u^{t+\Delta t_M}]} \\ &\approx \frac{\frac{1}{N_1} \sum_{i=0}^{N_1-1} (u_i^{t+\Delta t_M} - \tilde{u}_i^{t+\Delta t_M})^2}{\frac{1}{N_1-1} \sum_{i=0}^{N_1-1} (u_i^{t+\Delta t_M} - \bar{u})^2} = \lambda(u, \tilde{u}), \end{aligned} \quad (22)$$

where we require  $\lambda(u, \tilde{u}) \ll 1$ . In other words, since  $\mathbb{E}[(u^{t+\Delta t_M} - \tilde{u}^{t+\Delta t_M})^2] \geq \mathbb{E}^2[|u^{t+\Delta t_M} - \tilde{u}^{t+\Delta t_M}|]$ , we can bound only the first term and not consider the inequality in Eq. 18.

The resulting model approximation error in Eq. 22 is the same as proposed by Sobol in [31]. If we do not pass the interpolation test, we may try another interpolation method, or, if it is still possible, increase the number of samples  $N_1$ . Otherwise, we use the Monte Carlo method with  $N_1$  sample points.

**3.3. Metamodeling.** The metamodeling approach consists of substituting the expensive micro scale model with a metamodel, which produces an approximately similar output in a smaller amount of computing time. One way to construct such surrogate model is applying a data-driven method (Figure 4). First by sampling the multiscale model  $N_{meta}$  times, we obtained  $N_{meta} \cdot n_2$  samples of the micro model. This samples are used to construct a regression model  $P(\xi, u^t)$  by fitting the vector of uncertain parameters  $\xi$  and

initial condition  $u^t$ , which are outputs of the macro scale model at each macro time step. Then, when we actually sampling the results of the multiscale model (the right part of Figure 4), we do not need to run the expensive micro scale model, but predict its output using the regression model  $P(\xi, u^t)$ .

The mean value can be approximated by

$$\mathbb{E}[u^{t+\Delta t_M}(\xi)] \approx \frac{1}{N} \left( \sum_{j=0}^{N_{meta}-1} F^s(u_j^{t+n_1\Delta t_\mu}(\xi_j), \xi_j, \Delta t_M) + \sum_{j=N_{meta}}^{N-1} F^s(\tilde{u}_j^{t+n_1\Delta t_\mu}(\xi_j), \xi_j, \Delta t_M) \right), \quad (23)$$

where  $\tilde{u}_j^{t+n_1\Delta t_\mu}(\xi_j)$  denotes the results from the surrogate micro model.

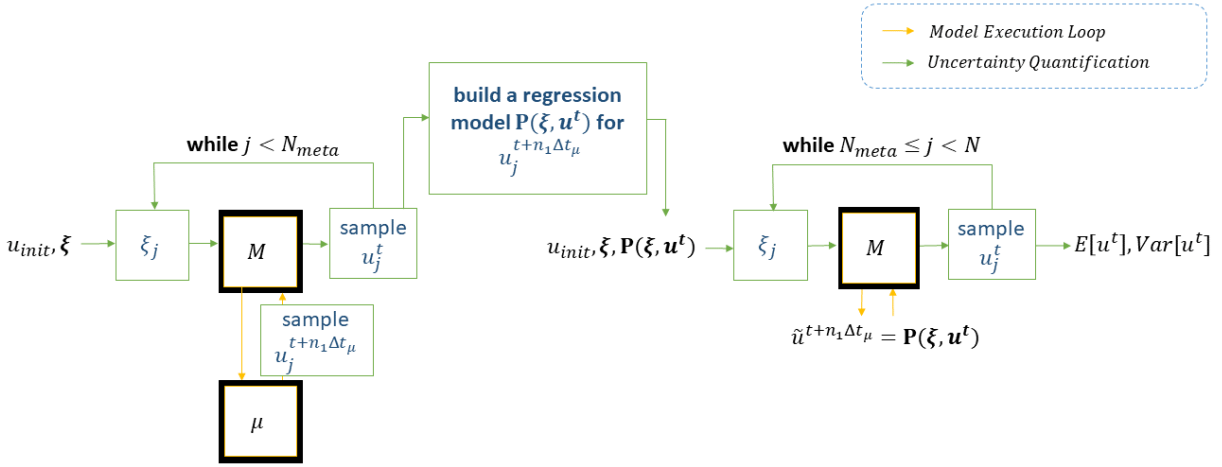


FIGURE 4. Metamodeling method

The computational time of running the metamodeling method for the multi-scale model is

$$T_{meta} = N_{meta}n_2(n_1\gamma + \beta) + Nn_2\beta + \varepsilon, \quad (24)$$

where  $\varepsilon$  is the computational time to build the metamodel.

**3.4. Stochastic Galerkin method.** In order to illustrate the combination of the semi-intrusive algorithm and the intrusive Galerkin method (Figure 5) for the single scale models, let us first represent uncertain inputs ( $\xi$ ) and solution ( $u^t$ ) via a truncated polynomial chaos (PC) expansion:

$$\begin{aligned} \xi_1 &= \sum_{i_1=0}^{\infty} \xi_{i_1} \Phi_{i_1}(\xi_1) \approx \sum_{i_1=0}^M \xi_{i_1} \Phi_{i_1}(\xi_1), \\ &\dots \\ \xi_n &= \sum_{i_n=0}^{\infty} \xi_{i_n} \Phi_{i_n}(\xi_n) \approx \sum_{i_n=0}^M \xi_{i_n} \Phi_{i_n}(\xi_n) \\ u^t(\xi) &= \sum_{i_1=0}^{\infty} \dots \sum_{i_n=0}^{\infty} u_{i_1 \dots i_n}^t \Phi_{i_1}(\xi_1) \dots \Phi_{i_n}(\xi_n) \\ &\approx \sum_{i_1=0}^M \dots \sum_{i_n=0}^{M-i_1 \dots i_{n-1}} u_{i_1 \dots i_n}^t \Phi_{i_1}(\xi_1) \dots \Phi_{i_n}(\xi_n) \end{aligned} \quad (25)$$



where  $\Phi_{i_j}$  is an orthogonal polynomial of order  $i_j$ ,  $u_{i_1 \dots i_n}$  are the PC coefficients, and  $M$  is the truncated power of the PC expansion. The total number of PC coefficients  $u_{i_1 \dots i_n}$  is equal to

$$P = \frac{(M+n)!}{M!n!}. \quad (26)$$

The mean value of the model response is equal to

$$\begin{aligned} \mathbb{E}[u^t(\xi)] &= \int_{(0,1)^n} u^t(\xi) w_1(\xi_1) \cdots w_n(\xi_n) d\xi_1 \cdots d\xi_n \\ &\approx \int_{(0,1)^n} \sum_{i_1=0}^M \cdots \sum_{i_n=0}^{M-i_1 \dots i_{n-1}} u_{i_1 \dots i_n}^t \Phi_{i_1}(\xi_1) \cdots \Phi_{i_n}(\xi_n) \\ &= \sum_{i_1=0}^M \cdots \sum_{i_n=0}^{M-i_1 \dots i_{n-1}} u_{i_1 \dots i_n} \langle \Phi_{i_1}(\xi_1), 1 \rangle \cdots \langle \Phi_{i_n}(\xi_n), 1 \rangle \\ &= u_{0 \dots 0} \end{aligned} \quad (27)$$

where  $w_i(\xi_i)$  denotes the  $i$ -th weight function, and we applied the following properties of the orthogonal polynomials:

$$\begin{aligned} \Phi_0(\xi) &= 1, \\ \text{and} \\ \langle \Phi_i(\xi), \Phi_j(\xi) \rangle &= \langle \Phi_i^2(\xi) \rangle \delta_{ij}. \end{aligned} \quad (28)$$

Variance of the model result can be estimated by

$$\begin{aligned} Var[u^t(\xi)] &= \underbrace{\mathbb{E}((u^t(\xi))^2)}_{\parallel} - \mathbb{E}^2(u^t(\xi)) = \sum_{i_1=0}^M \cdots \sum_{i_n=0}^{M-i_1 \dots i_{n-1}} (u_{i_1 \dots i_n}^t)^2 \langle \Phi_{i_1}^2(\xi_1) \rangle \cdots \langle \Phi_{i_n}^2(\xi_n) \rangle - u_0^2 \\ &\quad \sum_{i_1=0}^M \cdots \sum_{i_n=0}^{M-i_1 \dots i_{n-1}} (u_{i_1 \dots i_n}^t)^2 \langle \Phi_{i_1}^2(\xi_1) \rangle \cdots \langle \Phi_{i_n}^2(\xi_n) \rangle. \end{aligned} \quad (29)$$

The PC coefficients as a function of time can be found using the Galerkin projection. In the micro model, the process of updating the coefficients works as follows

$$\begin{aligned} u_{l_1 \dots l_n}^{t+\Delta t_\mu} &= \frac{1}{\langle \Phi_{l_1}^2(\xi_1) \rangle \cdots \langle \Phi_{l_n}^2(\xi_n) \rangle} \langle F^s( \sum_{i_1=0}^M \cdots \sum_{i_n=0}^{M-i_1 \dots i_{n-1}} u_{i_1 \dots i_n}^t \Phi_{i_1}(\xi_1) \cdots \Phi_{i_n}(\xi_n), \\ &\quad \sum_{i_1=0}^M \xi_{i_1} \Phi_{i_1}(\xi_1), \dots, \sum_{i_n=0}^M \xi_{i_n} \Phi_{i_n}(\xi_n), \Delta t_\mu), \\ &\quad \Phi_{l_1}(\xi_1), \dots, \Phi_{l_n}(\xi_n) \rangle \end{aligned} \quad (30)$$

The process of updating the coefficients on macro scale works is as follows

$$\begin{aligned} u_{l_1 \dots l_n}^{t+\Delta t_M} &= \frac{1}{\langle \Phi_{l_1}^2(\xi_1) \rangle \cdots \langle \Phi_{l_n}^2(\xi_n) \rangle} \langle F^s( \sum_{i_1=0}^M \cdots \sum_{i_n=0}^{M-i_1 \dots i_{n-1}} u_{i_1 \dots i_n}^{t+n_1 \Delta t_\mu} \Phi_{i_1}(\xi_1) \cdots \Phi_{i_n}(\xi_n), \\ &\quad \sum_{i_1=0}^M \xi_{i_1} \Phi_{i_1}(\xi_1), \dots, \sum_{i_n=0}^M \xi_{i_n} \Phi_{i_n}(\xi_n), \Delta t_M), \\ &\quad \Phi_{l_1}(\xi_1), \dots, \Phi_{l_n}(\xi_n) \rangle \end{aligned} \quad (31)$$

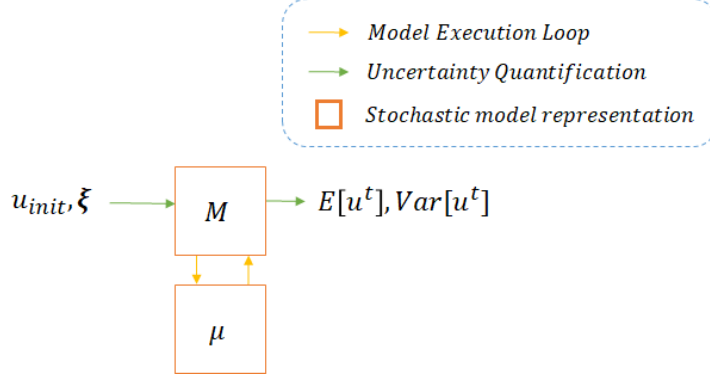


FIGURE 5. Diagram of the stochastic Galerkin method, where  $\mu$  and  $M$  denote stochastic representation of the micro and macro scales models.

The computational time of running the Galerkin method for a linear<sup>2</sup> multiscale model is

$$T_G = n_2(n_1(3P - 2)\gamma + (3P - 2)\beta). \quad (32)$$

To speed up the computations, we select different truncation power for the micro model  $M_1 < M$ . In this case, on the micro level we updated only the first  $P_1$  coefficients. Thus, the speed up is

$$T_G - T_{G^{M_1}} = n_2 n_1 3(P - P_1)\gamma. \quad (33)$$

Moreover, to compute sensitivity indices [30] using the Galerkin method [10], there is no need for additional model runs, and the indices are estimated directly from the PC coefficients.

**3.5. Coupling method (Coupled Intrusive & Non-intrusive methods).** The coupling method consists of applying intrusive and non-intrusive UQ methods for different single scale models (Figure 6). One can show that the intrusive Galerkin is an efficient approach, when we deal with a linear model, and can become prohibitive, in the case of non-linear operators [35]. Thus, the coupling approach is suitable, when the multiscale model contains linear and non-linear single scale models. Let us assume that  $\mu^s$  is a stochastic version of the linear micro scale model and  $M^s$  is a non-linear model with macro time scale. Thus, we can use Eq 30 for the PC coefficients update on the micro level. To update the coefficients on the macro scale, first we sample  $u_j^{t+n_1\Delta t_\mu}$  by

$$u_j^{t+n_1\Delta t_\mu} = \sum_{i_1=0}^M \cdots \sum_{i_n=0}^{M-i_1\cdots i_{n-1}} u_{i_1\cdots i_n}^{t+n_1\Delta t_\mu} \Phi_{i_1}(\xi_1^j) \cdots \Phi_{i_n}(\xi_n^j), \quad (34)$$

where the PC coefficients  $u_{i_1\cdots i_n}^{t+n_1\Delta t_\mu}$  are known from the run of micro model. Then, we apply the Monte Carlo method to find coefficient  $u_{l_1\cdots l_n}^{t+\Delta t_M}$ :

$$u_{l_1\cdots l_n}^{t+\Delta t_M} \approx \frac{1}{N} \sum_{j=0}^{N-1} F^s(u_j^{t+n_1\Delta t_\mu}(\xi_j), \xi_j, \Delta t_M) \Phi_{l_1}(\xi_1^j) \cdots \Phi_{l_n}(\xi_n^j) \quad (35)$$

The computational cost of the coupled approach is

$$T_{coupled} = n_2(n_1(3P - 2)\gamma + N\beta + P\varepsilon), \quad (36)$$

where  $\varepsilon$  indicates the computational cost of updating gPC coefficients on the macro scale.

<sup>2</sup>Note that we apply the Galerkin method only to linear models, since otherwise it can be highly non-trivial problem or computationally prohibitive. An example of application of the Galerkin method for UQ to a linear single scale model is shown in appendix A

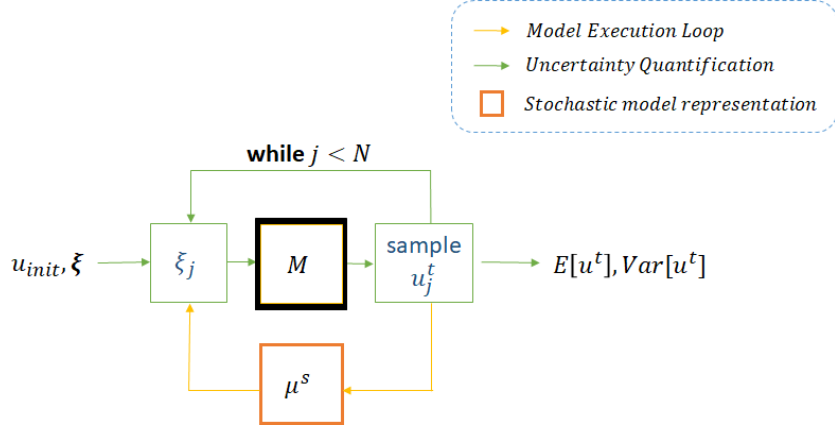


FIGURE 6. Diagram of coupling the intrusive Galerkin method and a non-intrusive generalized Polynomial Chaos

#### 4. CASE STUDY 1

The first case study is a 1D reaction-diffusion model with slow diffusion and fast reaction:

$$\begin{aligned}
 \frac{\partial u(x, t, \xi_1, \xi_2)}{\partial t} &= d(\xi_1) \frac{\partial^2 u(x, t, \xi_1, \xi_2)}{\partial x^2} + k(\xi_2) u(x, t), \text{ for } 0 \leq x \leq 1, t > 0 \\
 u(x, t = 0, \xi_1, \xi_2) &= u_0 = \sin(\pi(4x - 0.5)) + 1, \\
 u(x = 0, t, \xi_1, \xi_2) &= u(x = 1, t, \xi_1, \xi_2),
 \end{aligned} \tag{37}$$

where  $d(\xi_1)$  and  $k(\xi_2)$  are dimensionless diffusion and reaction coefficients with 10% uncertainty. Uncertainty was estimated for results from model simulation with  $n_1 = \frac{\Delta t_M}{\Delta t_\mu} = 100$  and  $n_1 = 1000$ . The mean value of  $\mathbb{E}[d(\xi_1)] = 4.05 \cdot 10^{-1}$ , and the mean value of the uncertain micro scale coefficient was set by  $\mathbb{E}[k(\xi_2)] = \frac{n_1 \mathbb{E}[d(\xi_1)]}{\Delta x^2}$  in the two experiments with different values of  $n_1$ .

We estimated the mean value and variance of the model results with different UQ methods: a sample-based method with the quasi-random Sobol sequence [23]; the semi-intrusive method<sup>3</sup> introduced above with  $\lambda(u, \tilde{u}) = 0.01$ ; metamodeling with the Gaussian Process Regression<sup>4</sup> [13, 34]; the stochastic Galerkin method (applied to the micro model) coupled with non-intrusive Polynomial Chaos approach (applied to the macro model); and the Galerkin method applied to the micro and macro models.

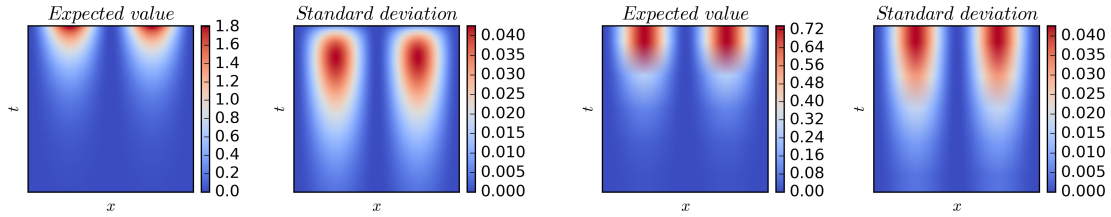
<sup>3</sup>The interpolation function  $f_{0,\dots,n-1}(\xi_n)$  from Eq. 16 was the griddata function with cubic method from Python scipy library [19] for the data interpolation in the semi-intrusive method.

<sup>4</sup>The GaussianProcessRegressor function from Python sklearn library [27] was used to obtain the metamodel of the micro model.

The UQ results from these methods were compared with the variance estimated from the analytical solution (Figure 7):

$$\begin{aligned}
 u(x, t, \xi_1, \xi_2) &= u^t = e^{tk(\xi_2)} \left( (u_0 - 1)e^{-16td(\xi_1)\pi^2} + 1 \right), \\
 \mathbb{E}(u^t) &= \frac{e^{tb_k} - e^{ta_k}}{t(b_k - a_k)} \left( \frac{u_0 - 1}{-16t\pi^2(b_d - a_d)} (e^{-16tb_d\pi^2} - e^{-16ta_d\pi^2}) + 1 \right), \\
 \text{Var}(u^t) &= \frac{e^{2tb_k} - e^{2ta_k}}{2t(b_k - a_k)} \left( \frac{(u_0 - 1)^2}{-32t\pi^2(b_d - a_d)} (e^{-32tb_d\pi^2} - e^{-32ta_d\pi^2}) \right. \\
 &\quad \left. + \frac{u_0 - 1}{-8t\pi^2(b_d - a_d)} (e^{-16tb_d\pi^2} - e^{-16ta_d\pi^2}) + 1 \right) - \mathbb{E}^2(u^t),
 \end{aligned} \tag{38}$$

where  $[a_k, b_k]$  and  $[a_d, b_d]$  are the ranges of the uniformly distributed random variables  $k(\xi_2)$  and  $d(\xi_1)$ .



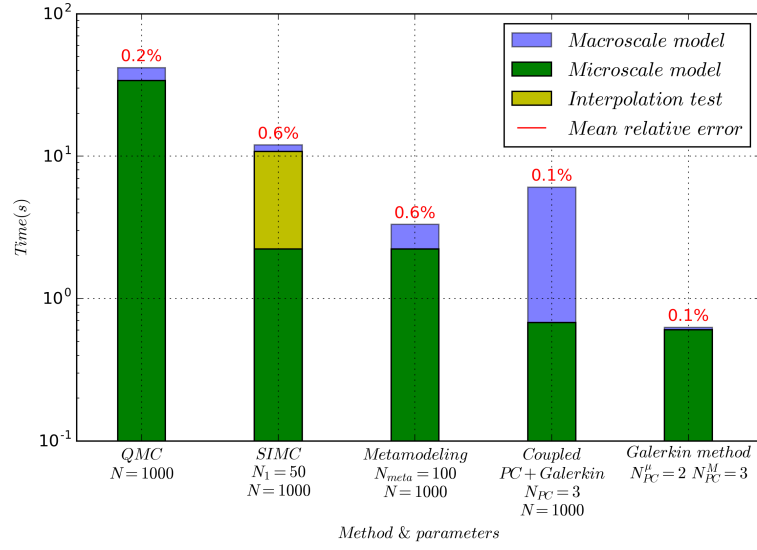
(A) The multiscale system with  $n_1 = 100$       (B) The multiscale system with  $n_1 = 1000$

FIGURE 7. Uncertainty Quantification result from the analytical solution

A comparison of the performance of different UQ approaches is presented in Figure 8 and Figure 9 with computational time, and difference (error) in the estimation of variance indicated above the columns of each of the methods. The error was estimated by

$$\epsilon_{method} = \frac{1}{N_x} \frac{1}{n_2} \sum_x \sum_t \frac{|(Var_{method})_x^t - (Var_A)_x^t|}{(Var_A)_x^t}, \tag{39}$$

where we sum up the difference between the result of variance from a method ( $Var_{method}$ ) and the UQ result from the analytical solution ( $Var_A$ ) at each time and space point and normalize the value by  $Var_A$  at this time and space point and divided by the dimension of the QoI  $N_x$  and number of macro time steps  $n_2$ .

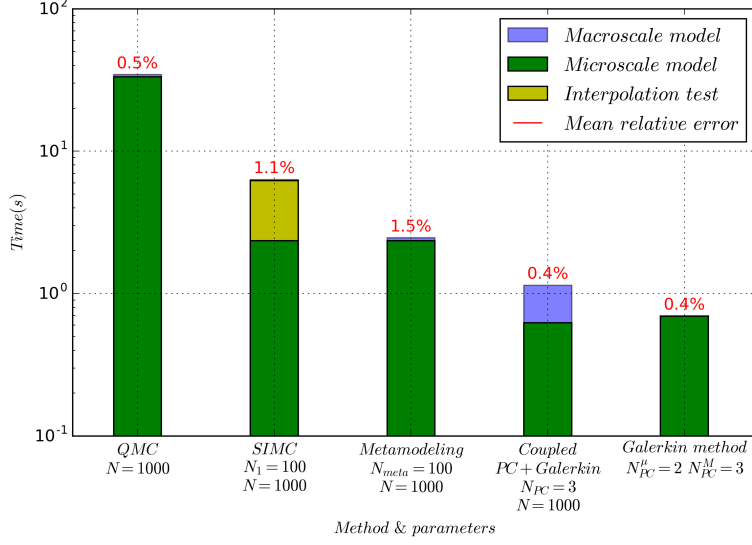
FIGURE 8. Comparison of UQ methods ( $n_1 = 100$ )TABLE 1. Computational time and speed-up in comparison with the QMC method ( $n_1 = 100$ )

Computational time	QMC	SIMC	Meta – modeling	Coupled	Galerkin
$T^{total}$ (s)	41.9	12.0	3.3	6.1	0.6
$\frac{T^\mu}{T^{total}} 100\%$	81.3%	90.3%	67.1%	11.2%	96.1%
$\frac{T^M}{T^{total}} 100\%$	18.7%	9.7%	32.9%	88.8%	3.9%
$\frac{T^{total}_{method}}{T^{total}_{QMC}} 100\%$	100.0%	28.6%	7.9%	14.5%	1.5%

TABLE 2. Computational time and speed-up in comparison with the QMC method ( $n_1 = 1000$ )

Computational time	QMC	SIMC	Meta – modeling	Coupled	Galerkin
$T^{total}$ (s)	34.5	6.3	2.5	1.1	0.7
$\frac{T^\mu}{T^{total}} 100\%$	96.7%	98.1%	95.7%	54.5%	99.5%
$\frac{T^M}{T^{total}} 100\%$	3.3%	1.9%	4.3%	45.5%	0.5%
$\frac{T^{total}_{method}}{T^{total}_{QMC}} 100\%$	100.0%	18.3%	7.1%	3.3%	2.0%

The comparison of the different UQ methods illustrates (Figure 8 and Figure 9) that we can significantly decrease the UQ computational time (Table 1 and Table 2), while, at the same time, keep the result of uncertainty estimation to be close to one from the analytical solution. This can be achieved by:

FIGURE 9. Comparison of UQ methods ( $n_1 = 1000$ )

- (1) Using the Monte-Carlo method separately on different time scales with lower number of samples for the micro model.
- (2) Building a metamodel of the expensive micro scale model.
- (3) When single scale model can be substituted by its stochastic representation, the intrusive Galerkin method can be coupled together with the non-intrusive Polynomial Chaos approach.

## 5. CASE STUDY 2

Our second example is a two-dimensional Gray-Scott model [26]. The model reproduces a complex pattern formation with a transition map studied in [15]. It consists of two coupled non-linear reaction-diffusion equations:

$$\begin{aligned} \frac{\partial u(t, x, y, \xi)}{\partial t} &= D_u \nabla^2 u + F(\xi_1)(1 - u) - uv^2, \\ \frac{\partial v(t, x, y, \xi)}{\partial t} &= D_v \nabla^2 v - (F(\xi_1) + k(\xi_2))v + uv^2, \end{aligned} \quad (40)$$

for  $x, y \subseteq [0, 2.5]^2$ , where  $D_u$  and  $D_v$  are dimensionless diffusion coefficients,  $F(\xi_1)$  is dimensionless feed rate, and  $k(\xi_2)$  is the dimensionless rate constant of the second reaction. We set diffusion to be a slow process with  $n_1 = 3$ . The system has Neumann boundary conditions and initial conditions [26] as follows

$$\begin{aligned} v(t = 0, x, y, \xi) &= \begin{cases} \frac{1}{4} \sin^2(4\pi x) \sin^2(4\pi y) & \text{if } x, y \subseteq [0.75, 1.75]^2 \\ 0 & \text{otherwise} \end{cases} \\ u(t = 0, x, y, \xi) &= \begin{cases} -2v(t = 0, x, y, \xi) + 1 & \text{if } x, y \subseteq [0.75, 1.75]^2 \\ 0 & \text{otherwise.} \end{cases} \end{aligned} \quad (41)$$

We assumed,  $F(\xi_1)$  and  $k(\xi_2)$  are model uncertain parameters with a uniform distribution and 1% variability, and  $D_u$  and  $D_v$  are constants, such that

$$\begin{aligned} D_u &= 2 \cdot 10^{-5}, \quad D_v = 10^{-5}, \\ \mathbb{E}[F(\xi_1)] &= 0.0385, \quad \mathbb{E}[k(\xi_2)] = 0.052. \end{aligned} \quad (42)$$

We estimated the statistics of the model results with five different UQ methods: Quasi-Monte Carlo (QMC) (Figure 10); semi-intrusive Monte Carlo method<sup>5</sup> (SIMC) with  $\lambda(u, \tilde{u}) = 0.5$ ; metamodeling with the Gaussian Process Regression; the intrusive Galerkin method (applied to the linear micro and macro models) coupled with the non-intrusive Polynomial Chaos (PC) approach (applied to the nonlinear micro model); and the Galerkin method applied to the micro and macro models.

The number of the QMC samples was selected according to a bootstrap estimation of the standard deviation of the estimated mean and standard deviation ( $s_{E[u]}$ ,  $s_{E[v]}$ ,  $s_{\sigma_u}$  and  $s_{\sigma_v}$  at Figure 10) [3]. The stopping criteria was such that the ratio between the sample standard deviation and mean value was less than 5%. Thus, the QMC samples size was set to 30000.

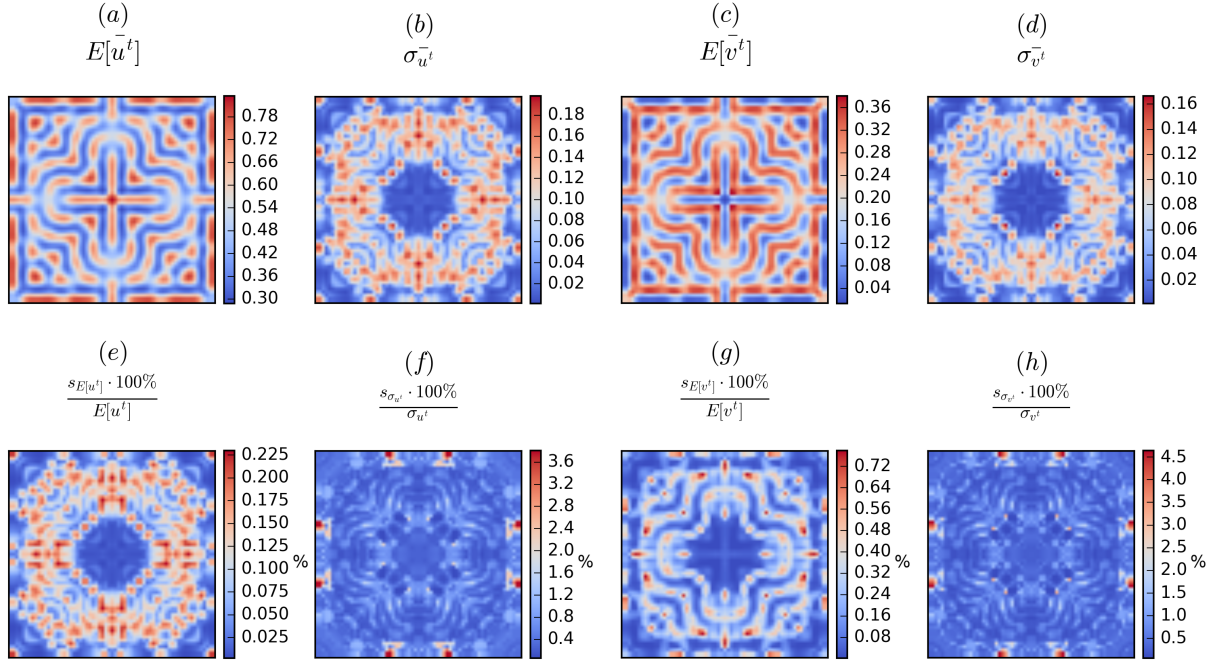


FIGURE 10. Uncertainty Quantification results from the QMC method with sample mean estimation of the expectation and standard deviation (plots (a) - (d)), and the ratio between the sample standard deviation and mean (plots (e) - (h))

The comparison of the performance of these approaches is presented in Figure 11 and Table 3. The mean relative error versus the results from the QMC approach (above the columns for each of the methods in Figure 11), calculated by

$$\epsilon_{method} = \frac{1}{2N_x N_y} \left( \sum_x \sum_y \frac{|(Var(u^{t_{end}})_{method})_{x,y} - (Var(u^{t_{end}})_{QMC})_{x,y}|}{(Var(u^{t_{end}})_{QMC})_{x,y}} + \sum_x \sum_y \frac{|(Var(v^{t_{end}})_{method})_{x,y} - (Var(v^{t_{end}})_{QMC})_{x,y}|}{(Var(v^{t_{end}})_{QMC})_{x,y}} \right), \quad (43)$$

<sup>5</sup>The interpolation function  $f_{0,\dots,n-1}(\xi_n)$  from Eq. 16 was the griddata function with linear method from Python scipy library for the data interpolation in the semi-intrusive method. Note that the interpolation with the cubic method required much large sample size ( $N_1$ ) in order to receive the same error as with the linear interpolation.

where we sum up the error at each point of the space grid of each of the species and divided by the number of this points ( $N_x \cdot N_y$ ).

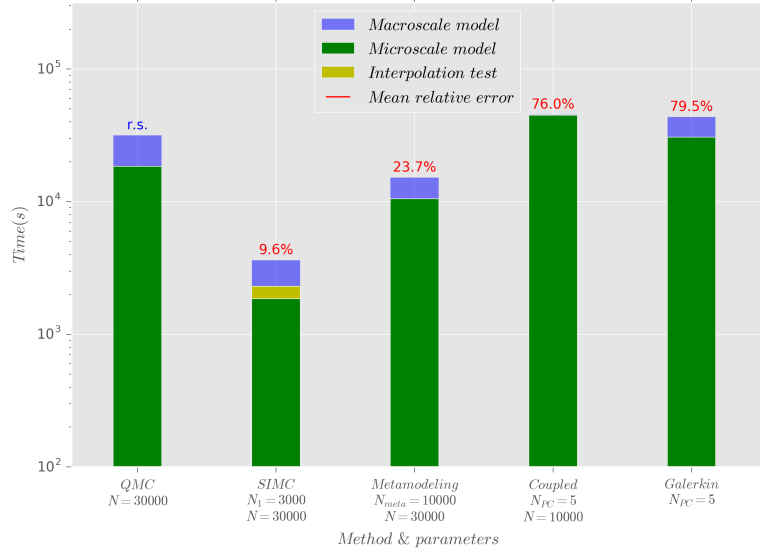


FIGURE 11. Comparison of the UQ methods performance, where "r.s" denotes the reference solution (the Gray-Scott model results)

TABLE 3. Computational time and speed-up in comparison with the QMC method (the Gray-Scott model results)

Computational time	<i>QMC</i>	<i>SIMC</i>	<i>Meta – modeling</i>	<i>Coupled</i>	<i>Galerkin</i>
$T^{total}$ (s)	31652.9	3627.1	15217.6	45341.5	43577.7
$\frac{T^\mu}{T^{total}} 100\%$	58.3%	63.4%	69.2%	99.05%	70.6%
$\frac{T^M}{T^{total}} 100\%$	41.7%	36.6%	30.8%	0.95%	29.4%
$\frac{T_{method}^{total}}{T_{QMC}^{total}} 100\%$	100.0%	11.5%	48.1%	143.2%	137.7%

The mean relative error in the variance estimation using the SIMC method with respect to the result from QMC is relatively small (Figure 11). Moreover, we reduce the computational time of UQ by applying this approach almost ten times (Table 3). The error from the result of the metamodeling approach is also not very large, however, we were need to increase significantly the sample size to obtain this error level. Thus, we may conclude that the Gaussian Process regression is not a good method to build a metamodel of a highly oscillating function like we have in this example. Moreover, the results obtained by the coupling and the intrusive Galerkin methods strongly deviate, because to build a stochastic representation of the function we need to take a much higher order of the PC expansion [24]. In addition, the intrusive Galerkin method is losing its efficiency in terms of computational cost, when applied to a non-linear model, since now all terms of the expansion in Eq. 30 preserve. In this case, the QMC method is more efficient in terms of computational time, because of a faster convergence.



## 6. CONCLUSIONS

We present three strategies to perform an efficient uncertainty quantification of a multiscale model by examining the coupling structure of the whole model. We show that knowledge of the model composition can be used in order to decrease the computational time of Uncertainty Quantification (UQ).

For instance, we can decrease the number of samples for the expensive micro scale model. We call such approach the semi-intrusive Monte Carlo (SIMC). Since one of the steps in this method is an interpolation test, we are able to control the accuracy of the results. Likewise, we can build a metamodel of the micro scale model before performing UQ, allowing us to compute an approximate model response without running the expensive micro model itself. Such surrogate model can be obtained using a data-driven approach, or substituting the original micro scale model by its computationally cheap version (in this case,  $N_{meta} = 0$ ). These methods can be used, when we deal with complex or unknown structure of single scale models. However, when one of the single scale model can be introduced by its stochastic representation, we can apply the intrusive Galerkin method to this single scale model, and be non-intrusive for other components of the multiscale model.

In the first case study, we tested the semi-intrusive approaches on an one-dimensional reaction-diffusion system. We show that applying the methods we can decrease computational time of UQ, and keep the error small. Moreover, we show two examples with different value of  $n_1$ , the number of micro time steps per one macro step. We observed that for the larger value of  $n_1$  the efficiency (in comparison to the non-intrusive Monte Carlo) of the semi-intrusive methods is higher than for smaller  $n_1$ . Thus, the strength of the semi-intrusive methods is more visible, when the cost of the micro scale model is much higher than the cost of the macro scale model, since the time for interpolation and to build the metamodel does not depend on  $n_1$ .

In the second case study, we applied the semi-intrusive UQ techniques to the Gray-Scott system in order to test that the algorithms are working for complex non-linear systems as well. We found that the coupled Galerkin method with non-intrusive Polynomial Chaos (PC) and the intrusive Galerkin method converge very slowly and require a high degree of the truncated PC expansion, what makes the methods non-efficient in terms of computational time. The metamodeling approach with the Gaussian Process regression also requires a large samples size to decrease a significant error appeared due the micro scale model approximation. However, the SIMC method produced a relatively small error, and dropped visibly the computational cost in comparison to the QMC approach. Moreover, for real world problems usually we are not given with any reference solution, and, usually, we cannot be aware about a significant error in the statistical values of the model response. The interpolation test tells us both: whether with the sample of size  $N_1$  we are able to describe the function of model uncertainty, and, whether we will not produce a large error using this interpolation function.

In the next step of this project, we will apply the performed SIMC method in order to estimate uncertainty in the 2D multiscale model of in-stent restenosis [7] with separated temporal scales.

## APPENDIX A. THE GALERKIN METHOD FOR A LINEAR MICRO SCALE MODEL

Suppose that as a result of time splitting we obtained that a single scale process can be described by a partial differentiation equation (PDE) of the form

$$\frac{\partial u(x, t, \xi)}{\partial t} = k(\xi) \mathcal{L}^1 u(x, t, \xi), \quad (44)$$

where  $\mathcal{L}^1$  is a single scale linear operator<sup>6</sup> acting in the  $x$ -variable,  $x$  and  $t$  are space and time variables, respectively,  $u(x, t, \xi)$  is the quantity of interest, and  $k(\xi)$  is an uncertain input with uniform distribution in  $[a_k, b_k]$  and  $-1 \leq \xi \leq 1$ .

First, we represent the random variable  $k(\xi)$  and uncertain solution  $u(x, t, \xi)$  with infinite series of orthogonal polynomials:

$$\begin{aligned} u(x, t, \xi) &= \sum_{n=0}^{\infty} u_n(x, t) \Phi_n(\xi), \\ k(\xi) &= k_0 + k_1 \Phi_1(\xi), \end{aligned} \quad (45)$$

where  $\Phi_n(\xi)$  is a Legendre polynomial of degree  $n$ . Now, we substitute the expansions into Eq. 44:

$$\begin{aligned} \sum_{i=0}^{\infty} \frac{\partial u_i(x, t)}{\partial t} \Phi_i(\xi) &= (k_0 + k_1 \Phi_1(\xi)) \mathcal{L}^1 \left( \sum_{i=0}^{\infty} u_i(x, t) \Phi_i(\xi) \right) \\ &= (k_0 + k_1 \Phi_1(\xi)) \sum_{i=0}^{\infty} \mathcal{L}^1(u_i(x, t)) \Phi_i(\xi) \\ &= k_0 \sum_{i=0}^{\infty} \mathcal{L}^1(u_i(x, t)) \Phi_i(\xi) + k_1 \Phi_1(\xi) \sum_{i=0}^{\infty} \mathcal{L}^1(u_i(x, t)) \Phi_i(\xi) \end{aligned} \quad (46)$$

We multiply both sides of the equation by  $\Phi_n$  and integrate, obtaining

$$\begin{aligned} \frac{\partial u_n(x, t)}{\partial t} \langle \Phi_n^2(\xi) \rangle &= k_0 \mathcal{L}^1(u_n(x, t)) \langle \Phi_n^2(\xi) \rangle + k_1 \sum_{i=0}^{\infty} \mathcal{L}^1(u_i(x, t)) \langle \Phi_1(\xi), \Phi_i(\xi), \Phi_n(\xi) \rangle \\ &= k_0 \mathcal{L}^1(u_n(x, t)) \langle \Phi_n^2(\xi) \rangle + k_1 (\mathcal{L}^1(u_{n-1}(x, t)) \langle \Phi_1(\xi), \Phi_{n-1}(\xi), \Phi_n(\xi) \rangle \\ &\quad + \mathcal{L}^1(u_{n+1}(x, t)) \langle \Phi_1(\xi), \Phi_{n+1}(\xi), \Phi_n(\xi) \rangle) \end{aligned} \quad (47)$$

Here we used two properties of the Legendre polynomials:

$$\langle \Phi_i(\xi), \Phi_j(\xi) \rangle = \langle \Phi_i^2(\xi) \rangle \delta_{ij}, \quad (48)$$

where  $\delta_{ij}$  is the Kronecker delta, and

$$\langle \Phi_1(\xi), \Phi_n(\xi), \Phi_l(\xi) \rangle = \langle \Phi_1(\xi), \Phi_{l-1}(\xi), \Phi_l(\xi) \rangle \delta_{l-1, n} + \langle \Phi_1(\xi), \Phi_{l+1}(\xi), \Phi_l(\xi) \rangle \delta_{l+1, n}. \quad (49)$$

Thus, it follows that

$$\begin{aligned} \frac{\partial u_n(x, t)}{\partial t} &= k_0 \mathcal{L}^1(u_n(x, t)) + \frac{k_1}{\langle \Phi_n^2(\xi) \rangle} \left( \mathcal{L}^1(u_{n-1}(x, t)) \langle \Phi_1(\xi), \Phi_{n-1}(\xi), \Phi_n(\xi) \rangle \right. \\ &\quad \left. + \mathcal{L}^1(u_{n+1}(x, t)) \langle \Phi_1(\xi), \Phi_{n+1}(\xi), \Phi_n(\xi) \rangle \right) \end{aligned} \quad (50)$$

#### ACKNOWLEDGEMENTS

This work is a part of the eMUSC (Enhancing Multiscale Computing with Sensitivity Analysis and Uncertainty Quantification) project. The authors gratefully acknowledge financial support from the Netherlands eScience Center.

Authors acknowledge fruitful discussions with L. Veen from the Netherlands eScience Center and G. E. Comi from the Scuola Normale Superiore di Pisa.

---

<sup>6</sup>The assumption that  $\mathcal{L}^1$  is a linear operator is a bit restrictive, however we still cover a number of important PDEs, such as diffusion, reaction, convection equations etc.

## REFERENCES

- [1] Rémi Abgrall and Pietro Marco Congedo. A semi-intrusive deterministic approach to uncertainty quantification in non-linear fluid flow problems. *Journal of Computational Physics*, 235:828–845, feb 2013.
- [2] Saad Alowayyed, Derek Groen, Peter V Coveney, and Alfons G Hoekstra. Multiscale computing in the exascale era. *Journal of Computational Science*, 2017.
- [3] G. E. B. Archer, A. Saltelli, and I. M. Sobol. Sensitivity measures, anova-like techniques and the use of bootstrap. *Journal of Statistical Computation and Simulation*, 58(2):99–120, 1997.
- [4] J Borgdorff, M Ben Belgacem, C Bona-Casas, Luis Fazendeiro, D Groen, O Hoenen, A Mizeranschi, JL Suter, D Coster, PV Coveney, et al. Performance of distributed multiscale simulations. *Phil. Trans. R. Soc. A*, 372(2021):20130407, 2014.
- [5] Joris Borgdorff, Jean-Luc Falcone, Eric Lorenz, Carles Bona-Casas, Bastien Chopard, and Alfons G. Hoekstra. Foundations of distributed multiscale computing: Formalization, specification, and analysis. *Journal of Parallel and Distributed Computing*, 73(4):465–483, apr 2013.
- [6] Joris Borgdorff, Mariusz Mamonski, Bartosz Bosak, Derek Groen, Mohamed Ben Belgacem, Krzysztof Kurowski, and Alfons G. Hoekstra. Multiscale computing with the multiscale modeling library and runtime environment. *Procedia Computer Science*, 18:1097 – 1105, 2013. 2013 International Conference on Computational Science.
- [7] Alfonso Caiazzo, David Evans, Jean-Luc Falcone, Jan Hegewald, Eric Lorenz, Bernd Stahl, Dinan Wang, Jörg Bernsdorf, Bastien Chopard, Julian Gunn, et al. A complex automata approach for in-stent restenosis: Two-dimensional multiscale modelling and simulations. *Journal of Computational Science*, 2(1):9 – 17, 2011.
- [8] Bastien Chopard, Jean-Luc Falcone, Alfons G. Hoekstra, and Joris Borgdorff. A framework for multiscale and multiscale modeling and numerical simulations. In *Lecture Notes in Computer Science*, pages 2–8. Springer Berlin Heidelberg, 2011.
- [9] Andrew J. Christlieb, Yuan Liu, and Zhengfu Xu. High order operator splitting methods based on an integral deferred correction framework. *Journal of Computational Physics*, 294:224 – 242, 2015.
- [10] Pham Luu Trung Duong, Wahid Ali, Ezra Kwok, and Moonyong Lee. Uncertainty quantification and global sensitivity analysis of complex chemical process using a generalized polynomial chaos approach. *Computers & Chemical Engineering*, 90:23–30, 2016.
- [11] W. E. *Principles of Multiscale Modeling*. Cambridge University Press, 2011.
- [12] Cyril Galitzine and Iain D. Boyd. An analysis of the convergence of the direct simulation monte carlo method. *Journal of Computational Physics*, 289:196–223, may 2015.
- [13] Alex Gorodetsky and Youssef Marzouk. Mercer kernels and integrated variance experimental design: Connections between gaussian process regression and polynomial approximation. *SIAM/ASA Journal on Uncertainty Quantification*, 4(1):796–828, 2016.
- [14] Derek Groen, Stefan J Zasada, and Peter V Coveney. Survey of multiscale and multiphysics applications and communities. *Computing in Science & Engineering*, 16(2):34–43, 2014.
- [15] Omri Har-shemesh, Rick Quax, Alfons G Hoekstra, and Peter M A Slood. Information geometric analysis of phase transitions in complex patterns: the case of the Gray-Scott reaction-diffusion model. *Journal of Statistical Mechanics: Theory and Experiment*, page 43301, 2016.
- [16] Alfons Hoekstra, Bastien Chopard, and Peter Coveney. Multiscale modelling and simulation: a position paper. *Phil. Trans. R. Soc. A*, 372(2021):20130377, 2014.
- [17] Willem Hundsdorfer and Jan G. Verwer. *Numerical Solution of Time-Dependent Advection-Diffusion-Reaction Equations*. Springer, 2010.
- [18] Ross H. Johnstone, Eugene T. Y. Chang, RÅmi Bardenet, Teun P. de Boer, David J. Gavaghan, Pras Pathmanathan, Richard H. Clayton, and Gary R. Mirams. Uncertainty and variability in models of the cardiac action potential: Can we build trustworthy models? *Journal of Molecular and Cellular Cardiology*, 96:49–62.
- [19] Eric Jones, Travis Oliphant, Pearu Peterson, et al. SciPy: Open source scientific tools for Python, 2001.
- [20] Sergey Karabasov, Dmitry Nerukh, Alfons Hoekstra, Bastien Chopard, and Peter V Coveney. Multiscale modelling: approaches and challenges. *Philosophical transactions. Series A, Mathematical, physical, and engineering sciences*, 2014.
- [21] O. P. Le Maître and Omar M. Knio. *Spectral Methods for Uncertainty Quantification*. Springer Netherlands, 2010.

- [22] A. Mittal, X. Chen, C. H. Tong, and G. Iaccarino. A flexible uncertainty propagation framework for general multiphysics systems. *SIAM/ASA Journal on Uncertainty Quantification*, 4(1):218–243, jan 2016.
- [23] William J. Morokoff and Russel E. Caflisch. Quasi-random sequences and their discrepancies. *SIAM Journal on Scientific Computing*, 15(6):1251–1279, 1994.
- [24] J. M. Pasini and T. Sahai. Polynomial chaos based uncertainty quantification in hamiltonian and chaotic systems. In *52nd IEEE Conference on Decision and Control*, pages 1113–1118, Dec 2013.
- [25] Grigoris Pavliotis and Andrew Stuart. *Multiscale methods: averaging and homogenization*. Springer Science & Business Media, 2008.
- [26] J E Pearson. Complex patterns in a simple system. *Science (New York, N.Y.)*, 261(5118):189–92, jul 1993.
- [27] Fabian Pedregosa, Gaël Varoquaux, Alexandre Gramfort, Vincent Michel, Bertrand Thirion, Olivier Grisel, Mathieu Blondel, Peter Prettenhofer, Ron Weiss, Vincent Dubourg, et al. Scikit-learn: Machine learning in python. *Journal of Machine Learning Research*, 12(Oct):2825–2830, 2011.
- [28] Peter MA Sloot and Alfons G Hoekstra. Multi-scale modelling in computational biomedicine. *Briefings in bioinformatics*, 11(1):142–152, 2009.
- [29] Ralph C Smith. *Uncertainty quantification: theory, implementation, and applications*, volume 12. Siam, 2013.
- [30] I. M. Sobol. Global sensitivity analysis indices for the investigation of nonlinear mathematical models. *Matematicheskoe Modelirovanie*, 19(11):23–24, 2007.
- [31] Ilya M Sobol. Global sensitivity indices for nonlinear mathematical models and their monte carlo estimates. *Mathematics and computers in simulation*, 55(1):271–280, 2001.
- [32] A. T. Sornborger. Higher-order operator splitting methods for deterministic parabolic equations. *International Journal of Computer Mathematics*, 84(6):887–893, 2007.
- [33] Xiaoliang Wan and George Em Karniadakis. An adaptive multi-element generalized polynomial chaos method for stochastic differential equations. *Journal of Computational Physics*, 209(2):617–642, nov 2005.
- [34] Bo Wang and Tao Chen. Gaussian process regression with multiple response variables. *Chemometrics and Intelligent Laboratory Systems*, 142(Supplement C):159 – 165, 2015.
- [35] Jeroen A. S. Witteveen and Hester Bijl. A monomial chaos approach for efficient uncertainty quantification in nonlinear problems. *SIAM Journal on Scientific Computing*, 30(3):1296–1317, 2008.
- [36] Dongbin Xiu. Fast numerical methods for stochastic computations: A review. *Communications in Computational Physics*, 5(2-4):242–272, 2 2009.